

Mixed Convection in a Vertical Heated Channel: Influence of the Aspect Ratio

Ameni Mokni^{1,2}, Hatem Mhiri¹, Georges Le Palec², Philippe Bournot²

Abstract—In mechanical and environmental engineering, mixed convection is a frequently encountered thermal fluid phenomenon which exists in atmospheric environment, urban canopy flows, ocean currents, gas turbines, heat exchangers, and computer chip cooling systems etc... . This paper deals with a numerical investigation of mixed convection in a vertical heated channel. This flow results from the mixing of the up-going fluid along walls of the channel with the one issued from a flat nozzle located in its entry section. The fluid-dynamic and heat-transfer characteristics of vented vertical channels are investigated for constant heat-flux boundary conditions, a Rayleigh number equal to $2.57 \cdot 10^{10}$, for two jet Reynolds number $Re=3 \cdot 10^3$ and 210^4 and the aspect ratio in the 8-20 range. The system of governing equations is solved with a finite volumes method and an implicit scheme. The obtained results show that the turbulence and the jet-wall interaction activate the heat transfer, as does the drive of ambient air by the jet. For low Reynolds number $Re=3 \cdot 10^3$, the increase of the aspect Ratio enhances the heat transfer of about 3%, however; for $Re=2 \cdot 10^4$, the heat transfer enhancement is of about 12%. The numerical velocity, pressure and temperature fields are post-processed to compute the quantities of engineering interest such as the induced mass flow rate, and average Nusselt number, in terms of Rayleigh, Reynolds numbers and dimensionless geometric parameters are presented.

Keywords—Aspect Ratio, Channel, Jet, Mixed convection

I. INTRODUCTION

IN mechanical and environmental engineering, mixed turbulent convection is a frequently encountered thermal fluid phenomenon, which exists in atmospheric environment, urban canopy flows, ocean currents, gas turbines, heat exchangers, nuclear reactors, solar collectors, and chemical vapor deposition reactors, and computer chip cooling systems etc... . In the early development of convective heat transfer studies, forced and natural convections were considered separately and the interaction between these two physical processes was ignored. Modern research combining forced

and natural convection was initiated in the 1960's and mainly based on experimental approaches.

Natural convection between heated vertical parallel plates is the most frequently used configuration in convection air cooling of electronic equipment. The passive character of cooling by natural convection makes it very attractive for applications in electronic devices. A review of the literature shows that laminar natural convection in vertical channel has been studied by several authors: Elenbaas [1] led the first experimental study which was used in the follow as reference solution. Bodoř and Österle [2] have obtained the first numerical solution of the natural convection in vertical channel. Their results were in good agreement with those Elenbaas. In order to increase the cooling requirements, researches for methods to improve the heat transfer parameters or to analyze standard configurations to carry out optimal geometrical parameters for a better heat transfer rate are crucial [3–9].

Heat transfer by natural convection from vertical plates with uniform wall temperature or heat flux has been extensively studied. G. Hugot [10] undertook an experimental study of the interaction of the boundary layers developing along two large parallel vertical plates. This study enabled him to measure the local heat transfer coefficients for various spacings and temperatures corresponding to Grashof numbers ranging from 5.10^5 to 2.10^{11} . The boundary layers interaction was defined by comparison with the single plate results. Moreover, information provided by the velocity, temperature profiles and their fluctuations lead to a better knowledge of the turbulence of the flow.

Katoh Y. et al. [11] studied experimentally turbulent natural convection flow and heat transfer in an asymmetrically heated vertical channel. The local velocity, the temperature values as well as heat transfer measurements were reported in their paper. Recently, Auletta and Manzo [12] carried out an experimental study on a channel-chimney system in order to elucidate the behaviour of the fluid flow and heat transfer. The channel is symmetrically heated and the chimney, located above the channel, is adiabatic. The presented results gave local measurements of the air temperature inside the channel and the adiabatic extension. They proposed some correlations connecting the local Nusselt number to the Rayleigh number for several geometrical configurations by varying the ratio height/width. A. Androzzzi et al. undertook a parametric study of a heated vertical parallel-plate channel owing an auxiliary plate at the inlet and two insulated extension plates attached to

A. Mokni is with the IUSTI UMR CNRS 6595, Technopole de Chateau-Gombert, 5 rue Enrico Fermi, 13013 Marseille Cedex 20 – France and with Unité de Thermique et Environnement, Ecole Nationale d'Ingénieurs de Monastir, Route de Ouardanine 5000 MONASTIR (TUNISIA) (phone: (+216) 97228560; e-mail: ameni26@yahoo.fr).

H. Mhiri, Jr., is with Unité de Thermique et Environnement, Ecole Nationale d'Ingénieurs de Monastir, Route de Ouardanine 5000 MONASTIR (TUNISIA)

G. Le Palec is with IUSTI UMR CNRS 6595, Technopole de Chateau-Gombert, 5 rue Enrico Fermi, 13013 Marseille Cedex 20 – France

Ph. Bournot is with IUSTI UMR CNRS 6595, Technopole de Chateau-Gombert, 5 rue Enrico Fermi, 13013 Marseille Cedex 20 – France

the heated walls at the exit [9]; later the same study was done with a channel–chimney system which walls are symmetrically heated at uniform heat flux[19]. They aimed to evaluate some geometric optimal configurations in terms of significant dimensionless geometric and thermal parameters.

The effect of aspect ratio with symmetrically heated channel or heated tube was also investigated in [10], [14-23]. The main purpose was at finding optimal configurations providing maximum heat transfer.

For the sake of completeness, few studies had concerned the mixed convection regime: we can mention Penot and al. [24] who proposed useful correlations to determine the flow rate, the fluid temperature, and the Nusselt number according to the heat flux density, the pressure difference and the Reynolds and Grashof numbers. M. Najam et al. [25] studied numerically the mixed convection in a “T” form cavity heated by the bottom. They showed the competition between natural and forced convection. The heat transfer was found maximal in the zone where the role of natural convection is more significant.

The present theoretical study is concerned with mixed convection in a heated vertical channel submitted to a constant heat flux with a co flow uniform injection issued from a vertical jet of fresh air (Pr=0.71). The influence of this forced additional jet is analyzed by using the low Reynolds number k-ε turbulence model. The flow is turbulent and steady. The present investigation deals with the effect of the channel aspect ratio on the mixed convective heat transfer parameters in channel. The optimal value of expansion ratio corresponding to the highest average Nusselt number is evaluated and a correlation in terms of Rayleigh number and extension ratio is proposed. The analysis is obtained for different Reynolds numbers, and channel aspect ratios.

II. ASSUMPTIONS AND GOVERNING EQUATIONS

The geometry of the problem investigated herein is described in Figure 1. We consider a vertical channel which simulates a chimney. A gas jet is issued from a flat nozzle located at the bottom of the channel. The chimney walls are subject to a constant heat flux which results in a mixed convection 2D-flow when the nozzle operates. The flow is assumed steady and incompressible. Mixed convection cases are considered by using the Boussinesq approximation in which the density varies linearly with temperature. Other thermo-physical quantities are assumed to be constant. Let us introduce the dimensionless variables defined by:

$$X = \frac{x}{H}, \quad Y = \frac{y}{H}, \quad U = \frac{u}{u_0}, \quad V = \frac{v}{u_0}, \quad P = \frac{(p + \rho g x)}{\rho u_0^2},$$

$$\theta = \frac{T - T_\infty}{\phi H} \lambda, \quad K = \frac{k}{u_0^2} \text{ and } E = \frac{\varepsilon H}{u_0^3} \quad (1)$$

Continuity equation:

$$\frac{\partial U}{\partial X} + \frac{\partial V}{\partial Y} = 0 \quad (2)$$

Momentum equation in X direction:

$$U \frac{\partial U}{\partial X} + V \frac{\partial U}{\partial Y} = -\frac{\partial P}{\partial X} + \frac{\partial}{\partial X} \left[\left(\frac{1}{\text{Re}_L} + \nu_t \right) \left[\frac{\partial U}{\partial X} \right] \right] + \frac{\partial}{\partial Y} \left[\left(\frac{1}{\text{Re}_L} + \nu_t \right) \left[\frac{\partial U}{\partial Y} \right] \right]$$

$$- \frac{2}{3} \frac{\partial K}{\partial X} + \frac{Ra}{\text{Pr Re}_L^2} \theta \quad (3)$$

Momentum equation in Y direction:

$$U \frac{\partial V}{\partial X} + V \frac{\partial V}{\partial Y} = -\frac{\partial P}{\partial Y} + \frac{\partial}{\partial X} \left[\left(\frac{1}{\text{Re}_L} + \nu_t \right) \left[\frac{\partial V}{\partial X} \right] \right] + \frac{\partial}{\partial Y} \left[\left(\frac{1}{\text{Re}_L} + \nu_t \right) \left[\frac{\partial V}{\partial Y} \right] \right]$$

$$- \frac{2}{3} \frac{\partial K}{\partial Y} \quad (4)$$

Energy equation:

$$U \frac{\partial \theta}{\partial X} + V \frac{\partial \theta}{\partial Y} = \frac{\partial}{\partial X} \left[\left(\frac{1}{\text{Re}_L \text{Pr}} + \frac{\nu_t}{\text{Pr}_t} \right) \left[\frac{\partial \theta}{\partial X} \right] \right] +$$

$$\frac{\partial}{\partial Y} \left[\left(\frac{1}{\text{Re}_L \text{Pr}} + \frac{\nu_t}{\text{Pr}_t} \right) \left[\frac{\partial \theta}{\partial Y} \right] \right] \quad (5)$$

Turbulent kinetic energy equation:

$$U \frac{\partial K}{\partial X} + V \frac{\partial K}{\partial Y} = \frac{\partial}{\partial X} \left[\left(\frac{1}{\text{Re}_L} + \frac{\nu_t}{\sigma_k} \right) \left(\frac{\partial K}{\partial X} \right) \right] +$$

$$\frac{\partial}{\partial Y} \left[\left(\frac{1}{\text{Re}_L} + \frac{\nu_t}{\sigma_k} \right) \left(\frac{\partial K}{\partial Y} \right) \right] - E + G_{DK} + G_{DB} \quad (6)$$

Rate of dissipation of turbulent kinetic energy equation:

$$U \frac{\partial E}{\partial X} + V \frac{\partial E}{\partial Y} = \frac{\partial}{\partial X} \left[\left(\frac{1}{\text{Re}_L} + \frac{\nu_t}{\sigma_\varepsilon} \right) \left(\frac{\partial E}{\partial X} \right) \right] +$$

$$\frac{\partial}{\partial Y} \left[\left(\frac{1}{\text{Re}_L} + \frac{\nu_t}{\sigma_\varepsilon} \right) \left(\frac{\partial E}{\partial Y} \right) \right] + C_{11} (G_{DK} + C_3 G_{DB}) \frac{E}{K} - C_2 \frac{E^2}{K} \quad (7)$$

Where : $G_{DK} = \nu_t \left(\frac{\partial U_i}{\partial X_j} + \frac{\partial U_j}{\partial X_i} \right) \frac{\partial U_i}{\partial X_j} - \frac{2}{3} K \delta_{ij} \frac{\partial U_i}{\partial X_j}$

and $G_{DB} = \frac{1}{\text{Fr}} \frac{\nu_t}{\text{Pr}_t} \frac{\partial \theta}{\partial X}$ (8)

E stands for the turbulent kinetic energy production due to shear, while G_{DK} is the turbulent kinetic energy production due to the mean velocity gradients, and G_{DB} is the turbulent kinetic energy production due to the buoyancy.

The standard k-ε model is used, so that constants are those given by Jones and Lauder [21]: $C_1 = 1.44$; $C_2 = 1.92$; $C_3 = 0.7$; $C_\mu = 0.09$; $\sigma_\varepsilon = 1.0$; $\sigma_k = 1.30$; $\text{Pr}_t = 1.0$.

The boundary conditions are the following:

At $Y = -\frac{e}{H}$; $U = 0$; $V = 0$; $\left(\frac{\partial \theta}{\partial Y} \right)_p = 1$, $K = 0$,

At $Y = \frac{e}{H}$; $U = 0$; $V = 0$; $\left(\frac{\partial \theta}{\partial Y} \right)_p = 1$, $K = 0$,

At $X = 0$; $-\frac{e}{H} < Y < -\frac{b}{2H}$; $p_g = -\frac{Q_1^2}{2}$, $\theta = 0$, $K = \frac{3}{2} I_1 U^2$,

$E = \frac{2eK^{0.5}}{b}$ (9)

$$-\frac{b}{2H} < Y < \frac{b}{2H}; U=1, v=0, \theta=0, K=0.001U,$$

$$E = \frac{2eK^{0.5}}{b}$$

$$\frac{b}{2H} < Y < \frac{e}{H}; P_g = -\frac{Q_1^2}{2}, \theta=0, K = \frac{3}{2}I_t U^2,$$

$$E = \frac{2eK^{0.5}}{b}$$

At $X=1; \frac{\partial U}{\partial X} = \frac{\partial V}{\partial X} = \frac{\partial \theta}{\partial X} = 0, P_g = 0, K = \frac{3}{2}I_t U^2, E = \frac{2eK^{0.5}}{b}$

Where I_t is the turbulence intensity. The inlet mass flow rates Q_1 and Q_2 are defined by:

$$Q_1 = \int_{b/2H}^{e/H} UdY = \int_{-e/H}^{-b/2H} UdY \text{ and } Q_2 = \int_{-b/2H}^{e/H} UdY \cdot \quad (10)$$

The governing equations reported above are discretized on a staggered, non-uniform Cartesian grid using a finite volume procedure. In this method, for stability considerations, scalar quantities P, θ, K and E are calculated at the centre (i,j) of the cells whereas, the velocity components (U and V) are computed on the faces of the cells ($i, j \pm 1/2$), ($i \pm 1/2, j$) as shown in Fig. 1.

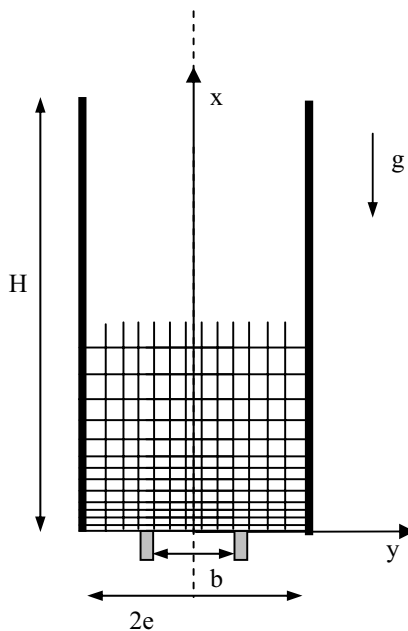


Fig.1. Coordinates system of the flow configuration

III. RESULTS AND DISCUSSION

The Results of the present investigation are carried out for air, $Pr = 0.71$, in the Rayleigh number based on the channel length is $2.57 \cdot 10^{10}$, the Reynolds number based on the jet velocity ranges between 3.10^3 and $2 \cdot 10^4$. The channel aspect ratio ranges from 8 to 20. We study the influence of the geometrical parameters, on the heat transfer enhancement. Computations deals with a symmetrically heated channel.

Preliminary tests were carried out to verify the accuracy of the numerical solution. The computations were performed first

for a simple channel - i.e. without gas injection from the nozzle - and numerical results were compared with the experimental ones published by A. Auletta et al. [12] (fig. 2). The resulting free convection problem was simulated with $H/2e = 2.5$ and , which corresponds to a Rayleigh number equal to $1.16 \cdot 10^{11}$. Results show the variation of the dimensionless temperature from the axis to the channel wall, for $X=0.5$ and $X=0.95$. Differences between experiments and numerical predictions are insignificant and they are mainly located at the centre of the channel ($X=0.5$): experimental wall temperature are a little superior than the calculated ones. This is due to the non uniformity of the imposed wall heat flux (because of the space between two successive heaters) and the heat losses caused by insufficient thermal insulation in experiments. At least, the use of thermocouples also modifies the flow structure, especially in the vicinity of the plates. All this explains that the discrepancies are higher near the wall.

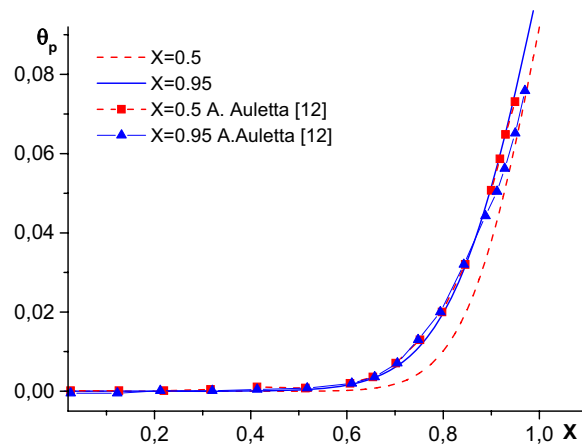


Fig.2. Temperature profiles for the configuration with $H/2e=2$. and $\Phi = 450$ W. Natural convection flow Comparison with experiments.

This part will be devoted to the analysis of the geometry on the flow development. Results are carried out for air, $Pr = 0.71$, the Rayleigh number is $Ra=2.57 \cdot 10^{10}$, two Reynolds numbers are considered $Re=3 \cdot 10^3$ and $Re=2 \cdot 10^4$ and for a channel aspect ratio $H/2e$ ranging from 8 to 20. Shown in Fig. 3 is the dimensionless mass flow rate, Q , as a function of the aspect ratio, $Ar=H/2e$, for the two values of Re . When the channel gap is wider, it produces a decrease of the pressure losses under the same driving force, (same Re and Ra), the mass flow rate increases. For low Reynolds number ($Re=3 \cdot 10^3$), the induced mass flow rate at the entry section decreases according to the jet aspect ratio due to the decrease at the entry section (fig.4.a): the jet flow is not powerful enough so that it ensures the drive of air from the whole entry section. When Re increases ($2 \cdot 10^4$), the air located at the vicinity of the entry section is aspirated into the channel under the action of the forced convection flow, a sensible mass flow rate increment is observed. The mass flow rate responds to an increasing function of Ar .

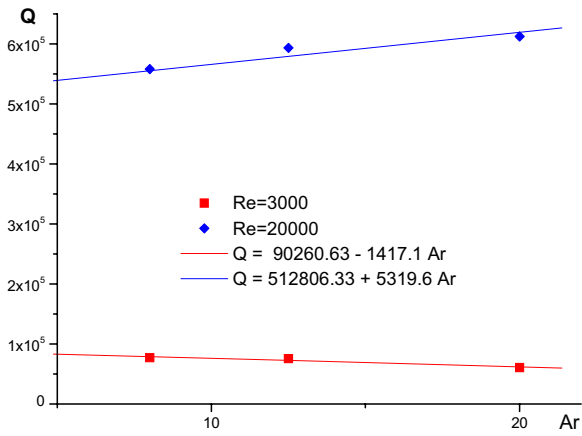
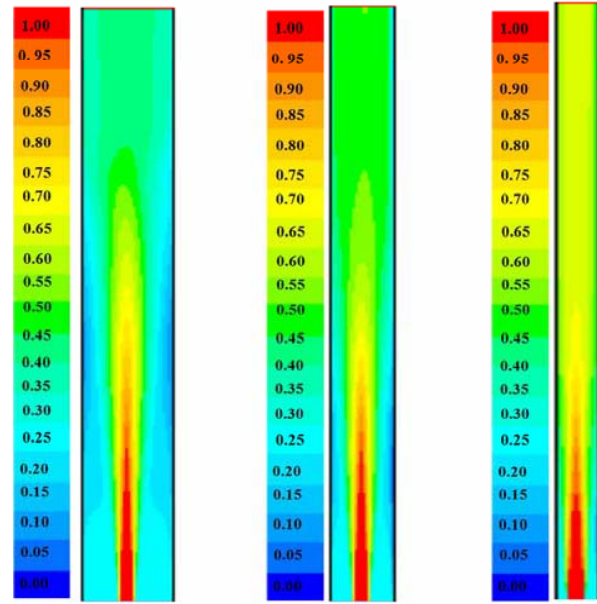
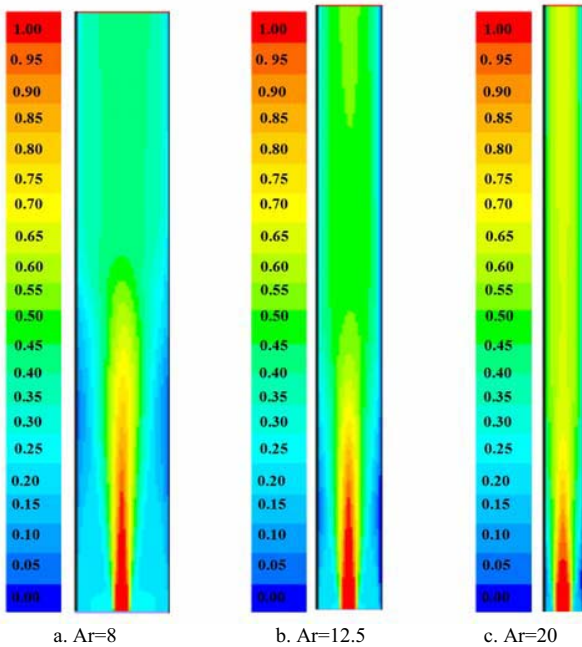


Fig.3. Natural convection and driven flow rate in the entrance section according to the channel aspect Ratio



a. Ar=8 b. Ar=12.5 c. Ar=20
 Fig.4. Streamlines for various aspect ratio $Ra=2.57 \cdot 10^{10}$ (b). $Re = 2 \cdot 10^4$



a. Ar=8 b. Ar=12.5 c. Ar=20
 Fig.4. Streamlines for various aspect ratio $Ra=2.57 \cdot 10^{10}$ (a). $Re = 3 \cdot 10^3$

Although the jet velocity and parietal heat flux are similar for all the treated cases, the flow does not occur in the same manner, in fact the channel walls influence the flow. For all the considered cases the jet goes further for low aspect ratio; for the significant aspect ratios, frictions within the adjacent walls slow down the flow. In contrast, when the channel gap is wider, the jet impact on the channel walls is weak; the flow behaves like a free jet: the surrounding fluid is aspirated towards the jet axis. This fact results in the creation of recirculation zones. (Fig.4)

Dependence of the skin friction defined by $C_f = \frac{2\tau_p}{\rho u_0^2}$ is shown in fig 5. the same flow behaviour is noted for all the aspects ratio considered: the skin friction increases at the immediate locality of the nozzle exit, it is then it decreases slightly, this corresponds to the area where the fluid flow falls off the wall and is sucked into the jet axis.

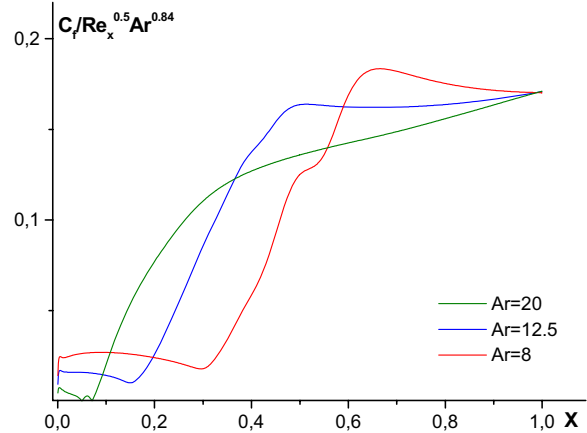


Fig. 5. streamwise evolution of the local friction coefficient $Ra = 2.57 \cdot 10^{10}$ (a). $Re=310^3$

Beyond this zone, the friction increases of advantage, the maximum friction value is reached in the impact zone. The boundary layer thickness increases, turbulence becomes intense, macroscopic agitation comes to be added to molecular agitation thus ensuring a significant momentum transport between the various fluid layers. Turbulences modify

instantaneous velocities and increase viscosity involving a loss of energy. From which it derives a larger friction coefficient. For $Ar = 20$, the jet offends the wall at the entrance area, the maximum friction zone is absent. Note that the ratio $\frac{C_f}{Re_x^{0.5} Ar^{0.84}}$ is approximately constant by the end of the channel for all the treated cases.

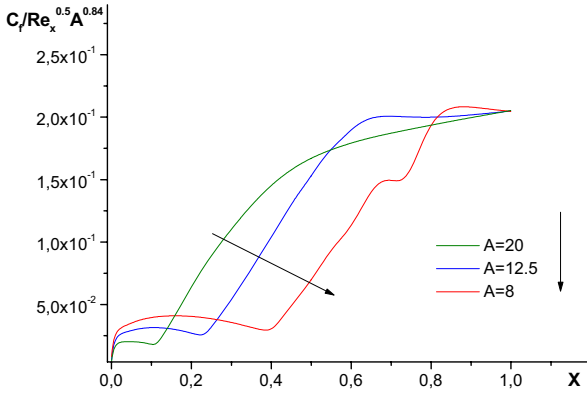


Fig. 5. streamwise evolution of the local friction coefficient $Ra = 2.5710^{10}$ (b). $Re=210^4$

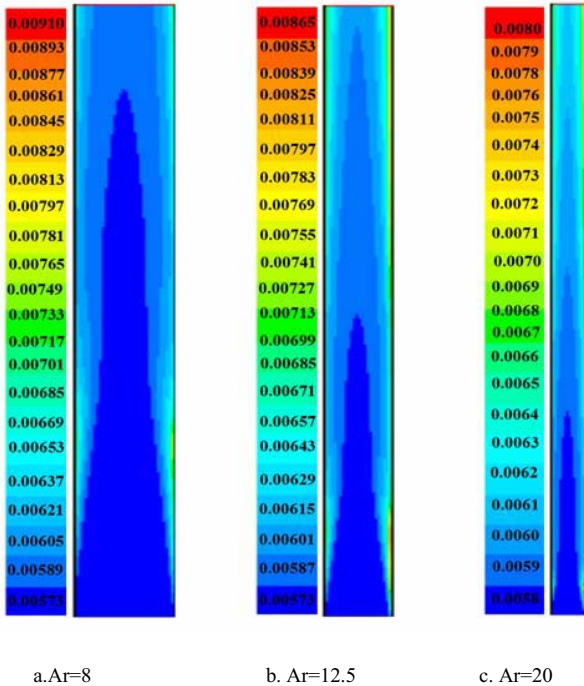


Fig.6. isotherms for various aspect ratio $Ra=2.57 \cdot 10^{10}$ (a). $Re = 3 \cdot 10^3$

The main important remark done from the isotherms depicted on fig 6. is that The effect of aspect ratio variation on the thermal and hydrodynamic fields is observed mainly at the entrance of the channel, it decreases when moving along the channel due to the hydrodynamic and thermal property of this flow.

The hot zones are moved into the flow direction for descending aspect ratio, these zones are larger for the lowest

aspect ratio and their intensity increases. These remarks are confirmed by the results of fig. 7. where the wall temperature is plotted for various aspect ratio. Indeed, the maximum dimensionless wall temperature increases, for descending channel aspect ratio, however; a reduction in the dimensionless wall temperature is observed at the outlet section (fig.7), Moreover, the decrease of the aspect ratio increases the location X_{max} of the maximum temperature value. This is due to the moving of the jet impact zone.

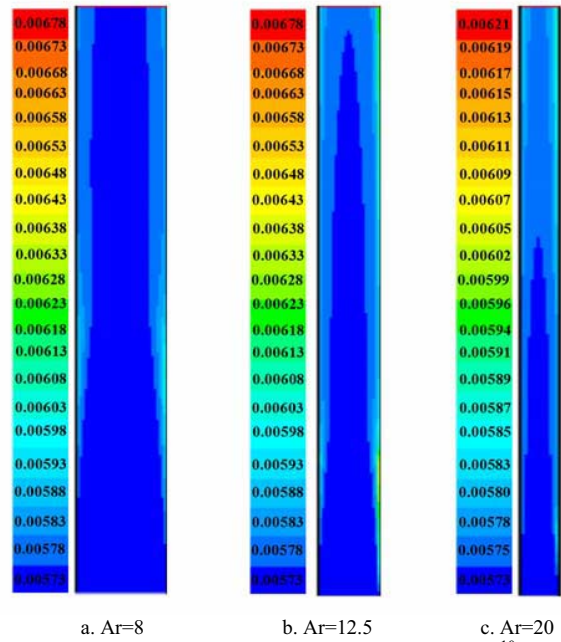


Fig. 6. isotherms for various aspect ratio $Ra=2.57 \cdot 10^{10}$ (b). $Re = 2 \cdot 10^4$

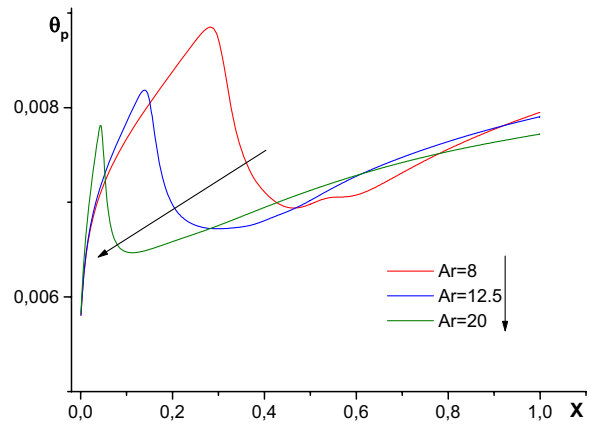


Fig.7. longitudinal wall temperature for various Aspect Ratio $Ra = 2.5710^{10}$ (a). $Re=310^3$

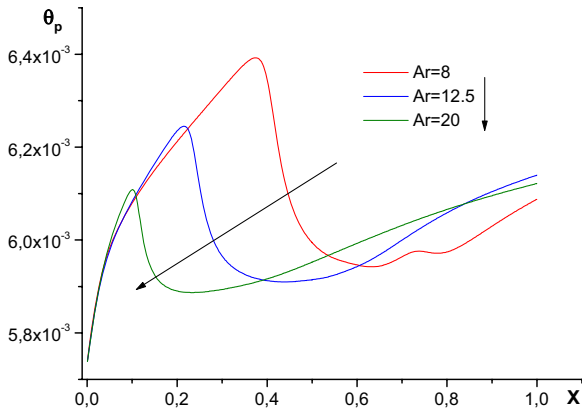


Fig.7. longitudinal wall temperature for various Aspect Ratio $Ra = 2.5710^{10}$ (b). $Re=210^4$

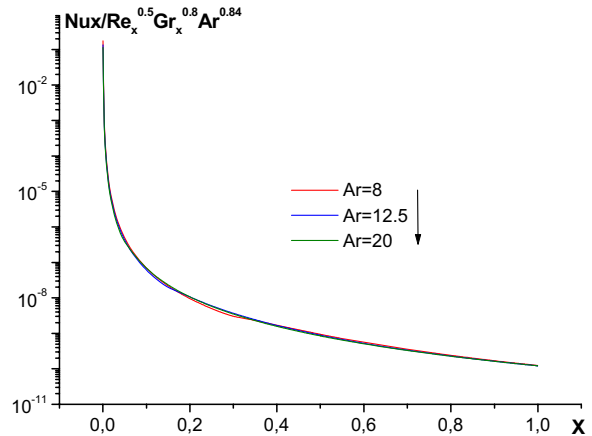


Fig.8. Local Nusselt number for various Aspect ratio $Ra = 2.5710^{10}$ (b). $Re=210^4$

Fig. 8 illustrates the Nusselt number values defined as $Nu_x = \frac{H}{\theta_p(X)}$ as a function of the longitudinal coordinate

X for various aspect ratio, at $Ra = 2.57 \cdot 10^{10}$ for $Re = 310^3$ in fig.8.a. and $Re = 210^4$ in fig. 8.b. We found that the Nusselt number decreases by increasing the aspect ratio of the pipe. The difference between the Nusselt numbers for different aspect ratio decreases as the Reynolds number increases. The Nusselt number values are higher at higher Ar, this trend is due to the greater mass flow rate that brings along a better heat transfer activity the maximum heat transfer corresponds to inlet section ; it decreases gradually. A second maximum is observed at the impact zone.

Other tests were made to evaluate the local Nusselt number for various Reynolds and Rayleigh numbers. Notice that the ratio $Nu_x / Re_x^{0.5} Ar^{0.84} Gr_x^{0.8}$ is almost invariant by the end of the channel for all the treated cases. So for all the analyzed aspect ratio, the following correlations are obtained:

$$Nu_x = 5.10^{-11} Pr^{0.33} Re_x^{0.5} Gr_x^{0.8} Ar^{0.84} \quad (11)$$

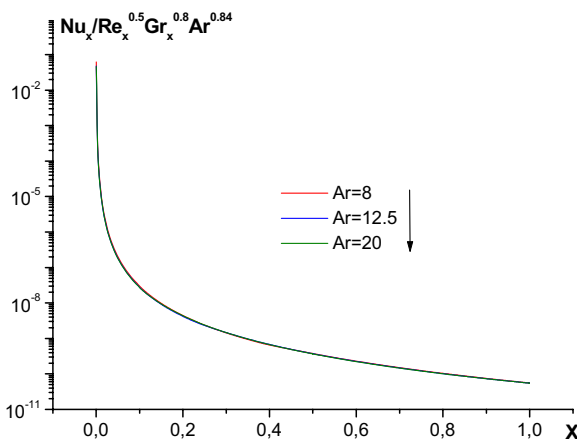


Fig. 8. Local Nusselt number for various Aspect ratio $Ra = 2.5710^{10}$ (a). $Re=310^3$

In order to quantify better the total heat exchange between the channel and the flow, let us study the evolution of the average Nusselt number, defined as:

$$Nu_m = \bar{Nu} = \frac{\bar{h}H}{\lambda}$$

where

$$\bar{h} = \frac{1}{H} \int_0^H h_x dx = \frac{1}{H} \int_0^H \frac{\varphi}{T_p - T_\infty} dx \quad (12)$$

The average Nusselt number is plotted on fig 9. according to the channel aspect Ratio for two Reynolds number. This figure shows a heat transfer enhancement for the two Reynolds number considered. Indeed a for a Reynolds number $Re = 3 \cdot 10^3$, the increase of the aspect Ratio enhance the heat transfer of about 3%, however for $Re = 2 \cdot 10^4$, the heat transfer enhancement is of about 12%.

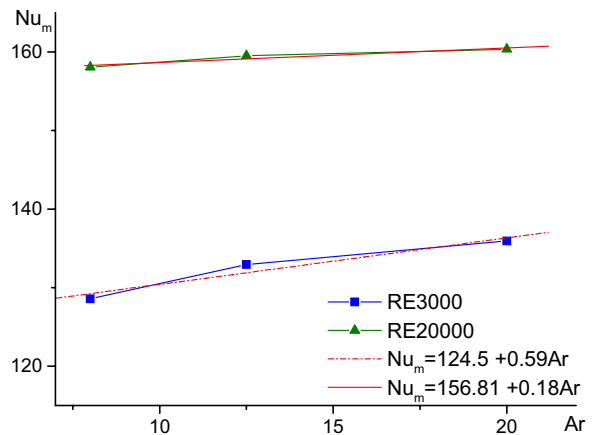


Fig. 9. Average Nusselt number according to the channel aspect ratio

IV. CONCLUSION

A numerical analysis of a heated vertical parallel-plate channel has been carried out. The channel walls are symmetrically heated at uniform heat flux giving rise to an upward convective flow of air through the conduit. Computations were performed for a Rayleigh number equal to $Ra=2.57 \cdot 10^{10}$, a Reynolds number ranging between $3 \cdot 10^3$ and $2 \cdot 10^4$, a channel aspect ratio ranging between 8 and 20. The aim is to evaluate some optimum configurations allowing the heat transfer enhancement. The mixed flow is obtained by using an ascending jet located at the entry section of the channel.

The obtained results show that an increase in the flow supports an effective cooling of the walls. The maximum heat transfer is reached at the entry area. We found that the Nusselt number decreases by increasing the aspect; this trend is due to the greater mass flow rate that circulates close to the channel walls, bringing along a better heat transfer activity. Correlations for dimensionless mass flow rate and average Nusselt numbers, in terms of Rayleigh number and dimensionless geometrical parameters, were proposed.

REFERENCES

- [1] W. Elenbaas, Heat Dissipation of Parallel Plates by Free convection, *Physica*, vol. 9, n° 1, pp.1-28, 1942
- [2] J.R. Bodoia and J.F. Osterle, The Development of Free Convection Between Heated Vertical Plates, *J. of Heat Transfer*, Trans. ASME, Series C, vol. 84, n°1, pp.40-44, 1962.
- [3] S.J. Kim, S.W. Lee, Air Cooling Technology for Electronic Equipment, CRC Press, Boca Raton, FL, 1996.
- [4] A. Bejan, Shape and Structure from Engineering to Nature, Cambridge University Press, New York, 2000.
- [5] G.A. Ledezma, A. Bejan, Optimal geometric arrangement of staggered vertical plates in natural convection, *ASME J. Heat Transfer* 119 pp. 700–708, 1997.
- [6] S. Sathe, B. Sammakia, A review of recent developments in some practical aspects of air-cooled electronic packages, *ASME J. Heat Transfer* 120 pp. 830–839, 1998.
- [7] A. Bejan, A.K. da Silva, S. Lorente, Maximal heat transfer density in vertical morphing channels with natural convection, *Numer. Heat Transfer A* 45, pp. 135–152, 2004.
- [8] A. Auletta, O. Manca, B. Morrone, V. Naso, Heat transfer enhancement by the chimney effect in a vertical isoflux channel, *Int. J. Heat Mass Transfer* 44 pp. 4345–4357, 2001.
- [9] A.K. da Silva, L. Gosselin, Optimal geometry of L- and C-shaped channels for maximum heat transfer rate in natural convection, *Int. J. Heat Mass Transfer* 48 pp. 609–620, 2005
- [10] A. Andreozzi, A. Campo, O. Manca, Compounded natural convection enhancement in a vertical parallel-plate channel, *Int. J. Thermal Sciences* 47 (6) (2008) 742–748.
- [11] Hugot G., Etude de la convection naturelle laminaire entre deux plaques planes verticales parallèles et isothermes, *Entropie* 46 pp. 55-66. 1972
- [12] M. Miyamoto, Y. Katoh, J. Kurima, H. Saki, Turbulent free convection heat transfer from vertical parallel plates. in *Heat Transfer*, eds C. L. Tien, V. P. Carey and J. K. Ferrell, Vol. 4. Hemisphere, Washington, DC, pp. 1593-1598. 1986
- [13] A. Auletta, O. Manca, Heat and fluid flow resulting from the chimney effect in a symmetrically heated vertical channel with adiabatic extensions, *International Journal of Thermal Sciences* 41 pp. 1101–1111. 2002.
- [14] A. Andreozzi, B. Buonomo, O. Manca, Thermal management of a symmetrically heated channel–chimney system, *International Journal of Thermal Sciences*, 48, pp. 475-487, 2009.
- [15] J.R. Dyer, The Development of Laminar Natural convective Flow in a Vertical Uniform Heat Flux Duct, *Int. J. Heat Mass Transfer*, vol.18, pp.1455-1465, 1975.
- [16] C.F. Hess and C.W. Miller, Natural Convection in a Vertical Cylinder subject to Constant Heat Flux, *Int. J. Heat Mass Transfer*, vol. 22, pp.421-430, 1979.
- [17] A. Bar-Cohen and W.M. Rohsnow, Thermally Optimum Spacing of Vertical Natural Convection Cooled, Parallel Plates, *J. Heat Transfer*, vol.116, pp.116-123, 1984.
- [18] F. Marcondes and C.R. Maliska, Treatment of the Inlet Boundary Conditions in Natural Convection Flows on open Ended Channels, *Numerical Heat Transfer*, Part B, vol.35, pp.317-345, 1999.
- [19] A. Auletta, O. Manca, B. Morrone, V. Naso, Heat transfer enhancement by the chimney effect in a vertical isoflux channel. *Int. J. Heat Mass Transfer* 44 pp. 4345–4357, 2001.
- [20] Y. Asako, H. Nakamura, M. Faghri, Natural convection in a vertical heated tube attached to a thermally insulated chimney of a different diameter. *ASME J. Heat Transfer*, pp.112 : 790–795, 1990.
- [21] A.G. Straatman, J.D. Tarasuk, J.M. Floryan, Heat transfer enhancement from a vertical, isothermal channel generated by the chimney effect., *ASME J. Heat Transfer*. 115 pp. 395–402, 1993.
- [22] A. Andreozzi, B. Buonomo, O. Manca, Numerical study of natural convection in vertical channels with adiabatic extensions downstream., *Numer. Heat Transfer A* (47):pp.1–22, 2005.
- [23] G.A. Shahin, J.M. Floryan, Heat transfer enhancement generated by the chimney effect in systems of vertical channel. *ASME J. Heat Transfer*, 121: pp.230–232, 1999.
- [24] F. Penot, A.M. Dalbert, convection naturelle mixte et forcée dans un thermosiphon vertical chauffé à flux constant., *International Journal of Heat and Mass Transfer* 26 (11) pp.1639-1647, 1983.
- [25] M. Najam, M. El Almi, M. Hasnaoui, A. Amahamid, Etude numérique de la convection mixte dans une cavité en forme de T soumis à un flux de chaleur constant et ventilé par le bas à l'aide d'un jet d'air vertical., *Compte Rendu de Mécanique*, 330 pp. 461–467, 2002.